

Conditional Deletion of PTH/PTHrP Receptor 1 in Osteocytes Abolishes Lactation-induced Alterations in Canalicular Pericellular Space and Increases Bone Microstructure Deterioration

Xiaoyu Xu¹, Yilu Zhou¹, Rosa M. Guerra², Yongqiang Vincent Jin¹, Yuanhang Li¹, Wonsae Lee¹, Tala Azar¹, Kira Lu¹, Liyun Wang², X. Sherry Liu¹

¹McKay Orthopaedic Research Laboratory, University of Pennsylvania, Philadelphia, PA. xiaoyu.xu@penmedicine.upenn.edu

²Center for Biomechanical Engineering Research, University of Delaware, Newark, DE.

Disclosures: All authors have nothing to disclose.

INTRODUCTION: Pregnancy and lactation are unique physiological events for women that induce significant changes in maternal calcium and bone metabolism. Due to the demands of infant growth and milk production, the maternal skeleton experiences substantial mineral loss and structural deterioration during lactation, followed by partial recovery after weaning [1,2]. Osteocytes, the orchestrators of bone mass maintenance, have been considered to play a key role in lactation-induced maternal mineral metabolism by resorbing their surrounding bone matrix through perilacunar/canalicular remodeling (PLR) [3], resulting in a transient increase in dimensions of the lacunar canalicular system (LCS) in maternal bone during lactation. Moreover, our previous study suggested that increased dimensions of osteocyte LCS driven by PLR would amplify the transductions of mechanical and biochemical signals to osteocytes, leading to increased osteocyte mechanosensitivity, which in turn enhances the mechanical adaptation of the maternal skeleton to maintain its load-bearing function [4-5] (Fig. 1A). However, the exact role of PLR in regulating maternal bone adaptations during lactation is still unclear. Therefore, the objective of this study was to investigate the impact of PLR on lactation-induced changes in the ultrastructure of the LCS and microstructure of the maternal bone. We hypothesized that abolishing osteocyte PLR would prevent changes in the pericellular matrix and LCS dimensions, leading to more significant bone loss and bone microstructure deterioration during lactation. In order to abolish lactation-induced PLR, PTH/PTHrP Receptor 1 (PPR) was conditionally deleted in osteocytes using a *Dmp1-Cre; PPR^{fl/fl}* mouse model. Skeletal morphology, osteocyte LCS dimension, and pericellular ultrastructure were examined at different stages of reproduction to elucidate the role of osteocyte PLR in lactation-induced maternal alternations.

METHODS: All animal experiments were IACUC approved. **Animals:** Female C57BL6 mice with osteocyte deletion of PPR (cKO: 14kb-*Dmp1-Cre; PPR^{fl/fl}*) and the matched wildtype controls (WT: *PPR^{fl/fl}* littermates) were both randomly assigned to three groups: Virgin, Lactation, and Post-weaning (n = 4-6 per group for both cKO and WT). Lactation and Post-weaning mice were mated at 11 and 9 weeks old, respectively, and underwent 3 weeks of pregnancy followed by 12 days of lactation. To ensure consistent suckling intensity, litter sizes were normalized to 5-6 pups per mother within 48 hours after birth. Post-weaning mice were allowed to recover for 14 days after 12 days of lactation. At 16 weeks old, Lactation and Post-weaning mice were euthanized with the age-matched Virgin mice. **Histomorphometry:** Longitudinal sections (6- μ m) were prepared from the paraffin-embedded tibia (right) and subjected to Photon silver nitrate staining to evaluate the LCS dimensions in all groups (n = 3-4 per group; n = 30-35 lacunae per sample). **Transmission electronic microscope (TEM):** Bone marrow was washed out from the tibia (left) immediately after dissection. After fixation, the tibial midshaft was transversely cut into 1mm thick sections using a low-speed saw and processed for TEM imaging to analyze the ultrastructure of canalliculi (290-300 canalliculi per group). A Matlab program was developed to evaluate the pericellular area and cell process area of the osteocyte dendrites and the total canalicular area. **μ CT imaging:** The trabecular bone of the lumbar vertebra L4 was scanned and analyzed using a microCT 45 (Scanco; 7.5 μ m voxel size). Microstructural parameters, including bone volume fraction (BV/TV), trabecular thickness (Tb.Th), SMI, and connectivity density (Conn. D) were acquired. **Statistics:** One-way ANOVA with Bonferroni correction was used to detect the difference in relevant parameters across Virgin, Lactation, and Post-weaning groups. Significant differences were considered when $p < 0.05$.

RESULTS: In WT mice, 12-day lactation resulted in 20% and 9% greater lacunar area and perimeter, respectively, which returned to baseline levels as in Virgin mice 14 days after weaning (Fig. 1B&C). These lactation-induced alternations were not found in mice lacking osteocyte PPR (Fig. 1B-D). Although the number of canalliculi per lacuna remained consistent across Virgin, Lactation, or Post-weaning for both WT and cKO mice (Fig. 1D), the ultrastructure of canalliculi adapted differently between WT and cKO mice during lactation. The pericellular area around osteocyte dendrites increased by 48% in WT lactating mice (Fig. 1E), resulting in a 30% increase in total canalicular area compared to Virgin mice (Fig. 1G). Following the weaning period, the recovery of canalliculi ultrastructure in WT mice was evidenced by the significant reduction in the pericellular area 14 days after weaning (Fig. 1E). Unlike the alternation in WT mice, deleting PPR in osteocytes mitigated lactation-induced increases in pericellular and canalicular areas (Fig. 1E&G). Moreover, the post-weaning recovery observed in WT did not appear in cKO mice, as both pericellular and canalliculi areas remained elevated after 14 days post weaning (Fig. 1E&G). The dendrite process area remained at similar levels at different reproductive stages in WT and cKO mice (Fig. 1F). At the tissue level, cKO mice displayed greater bone loss and microstructure deterioration during lactation than WT mice, demonstrated by significant reductions in BV/TV (-48%), Tb.Th (-26%), Conn.D (-34%), and a higher SMI (2.5 in cKO vs. 2.23 in WT) in cKO relative to WT (Fig. 1H-K). Nevertheless, both WT and cKO mice fully recovered in bone microstructure post weaning (Fig. 1H-K).

DISCUSSION: Our results demonstrated the important role of osteocyte PLR in mediating alternations of the LCS ultrastructure and maternal bone microstructure in response to lactation. By deleting PPR in osteocytes, lactation-induced osteocyte PLR activities were abolished in the mouse maternal skeleton, demonstrated by the unchanged lacunar area and perimeter across different reproductive statuses in the cKO mice. TEM results provided further evidence of the functions of osteocyte PLR in altering the pericellular matrix of osteocyte dendrites and dimensions of canalliculi during lactation. According to the LCS fluid flow model established by Weinbaum *et al.* [6], the enlarged LCS and pericellular fluid space could contribute to increased flow-mediated mechanical stimulation and enhanced mechano-signals on osteocytes and their processes when subjected to loading, thus enhancing bone's mechano-responsiveness during lactation. This may partially explain the accelerated bone loss in lactating cKO mice with lactation-induced osteocyte PLR significantly inhibited.

SIGNIFICANCE: This is the first study that quantified the lactation-induced alterations in canalliculi ultrastructure and demonstrated active remodeling of the pericellular matrix surrounding osteocyte dendrites during lactation and post-weaning. Future studies will continue to elucidate the critical roles of osteocyte PLR in regulating the balance between mineral resorption and mechanical integrity of the maternal skeleton.

REFERENCES: [1] Kovacs, *Physiol Rev*, 2015; [2] Liu X *et al.*, *Biomech*, 2019; [3] Qing H *et al.*, *JBRM*, 2012; [4] Lai X *et al.*, *Bone*, 2021; [5] Li Y *et al.*, *Bone*, 2021; [6] Weinbaum *et al.*, *J Biomech*, 1994.

ACKNOWLEDGEMENTS: NIH/NIAMS R01-AR077598, P30-AR069619.

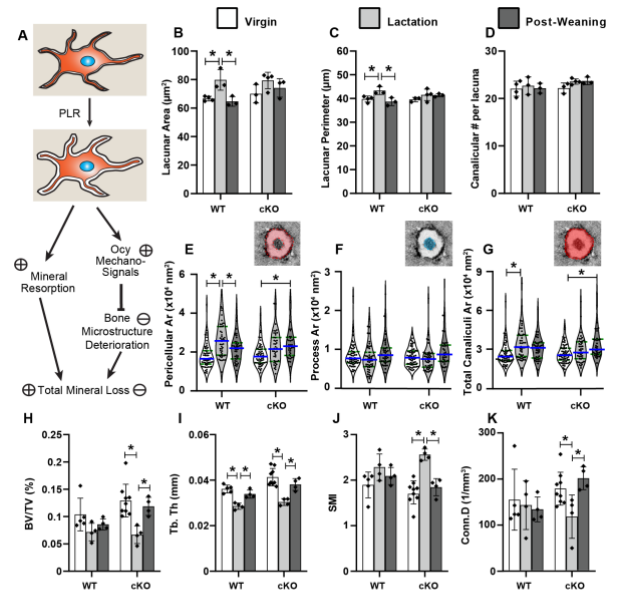


Figure 1 (A) Schematic diagram of osteocyte PLR regulation of mineral resorption and bone mechanical integrity. (B) Lacunar area, (C) lacunar perimeter, and (D) canalliculi number per lacuna derived from Ploton silver nitrate staining images of cKO and WT mice with different reproductive statuses. (E) Pericellular area of Ocy dendrite processes (area between the two red dashed lines), (F) process area (central area highlighted in blue), and (G) total canalliculi area (the area highlighted in red) derived from TEM images of tibial cortical bone of cKO and WT mice with different reproductive statuses. (H-K) L4 trabecular bone morphometry by μ CT (7.5 μ m) in cKO and WT Virgin, Lactation, and Post-weaning mice. Asterisk (*) indicates a significant difference among Virgin, Lactation, and Post-weaning of cKO or WT mice by one-way ANOVA ($p < 0.05$).